

Neural Net Based Torque Sensor Using Birefringent Materials

Dukki Chung

Dept. of Electrical Engineering and Applied Physics
Case Western Reserve University
10900 Euclid Avenue
Cleveland, Ohio 44106
Phone: (216)368-8871
E-mail: dkc6@po.cwru.edu

Francis L. Merat

Dept. of Electrical Engineering and Applied Physics
Case Western Reserve University
10900 Euclid Avenue
Cleveland, Ohio 44106
Phone: (216)368-4572
FAX: (216)368-6039
E-mail: flm@po.cwru.edu

Fred M. Discenzo

Rockwell Automation, Advanced Technology
24800 Tungsten Road
Cleveland, Ohio 44117
Phone: (216)266-6759

James S. Harris

Rockwell Automation, Advanced Technology
24800 Tungsten Road
Cleveland, Ohio 44117
Phone: (216)266-1016

Abstract

Photoelasticity can be used to accurately measure surface strains or stresses in a part or structure. In this paper we describe the use of a photoelastic transducer and neural net image processing to estimate the torque of stationary and rotating shafts. A strain sensitive (photoelastic) plastic cylinder is attached to the shaft and illuminated by polarized light. As the shaft torque varies the photoelastic plastic displays the corresponding shaft strain as a 2-D fringe pattern when viewed through an optical polarizer. The strain that causes this observed optical pattern is a complex function of the torque applied to the shaft. In this paper, we describe the use of neural net image processing to determine function value to realize an optical torque sensor. A CCD camera/image processing system was used to acquire and process the optical patterns. A neural net torque estimator was trained with these fringe patterns and tested against a laboratory strain gauge torque sensor. Our experiments show that the neural net torque estimator can accurately estimate (to within a few percent) the applied torque for both static and slowly rotating (<20 rpm) shafts.

1. Introduction

Transparent photoelastic materials such as some polymeric plastics are optically isotropic under normal conditions but become birefringent when stress is applied. This birefringent phenomenon was first observed in the nineteenth century [1]. Birefringent materials have the ability to resolve an impinging light vector into components along the principal strain axes and to transmit each component with a different velocity. The relative phase retardation between these two beam components (designated 1 and 2) is given by

$$\delta = t(n_1 - n_2) = tE(\epsilon_1 - \epsilon_2) \quad (1)$$

where t is the thickness of the photoelastic material, n_i is the index of refraction for the i -th component, ϵ_i is the strain intensity along the i -th axis, and E is a function of the material called the strain-optical coefficient [2]. When linearly polarized light passes through a birefringent plastic the relative phase retardation will be given by Equation (1). The light exiting the plastic can be passed through a linear polarizer to convert the phase retardation into an intensity given by

$$I = a^2 \sin^2 2(\beta - \alpha) \sin^2(\pi\delta/\lambda) \quad (2)$$

where $(\beta - \alpha)$ is the angle between the analyzer and the principal strain axis. The analyzer can be used to measure the principle strain direction by rotating the analyzer until the intensity becomes zero, i.e. $\alpha = \beta$. Many variants on this technique are possible. The light may be reflected back through the plastic to double the retardation. Circularly polarized light may be used to eliminate any dependence upon the principal strain axis. Typically a monochromatic light source is used to produce an isochromatic intensity pattern. A white light source can also

be used with the resulting color indicating the relative phase retardation and, therefore the strain [2]. However, a narrow band or monochromatic light source produces more clearly visible fringes for high fringe orders.

When polarized light passes through a stressed photoelastic material and is viewed through a polarizer, colorful fringe patterns are observed. These two-dimensional optical fringe patterns have been widely used for stress analysis [1, 2]. However, these methods typically need human interpretation for proper analysis. In this paper, a novel approach using neural nets is proposed for analyzing the visible fringe patterns of a shaft coupler incorporating birefringent plastic to make a very accurate shaft torque sensor.

Neural net models have been used for many years to mimic the functional abilities of biological neurons. These models consist of nonlinear processing elements operating in parallel and arranged similar to biological neural nets. Processing elements (nodes) are connected via weights (synapses) that are typically adapted during training phase. Incoming signals (stimulus) are passing through the weights and multiplied by the weights, and summed at the processing elements, or nodes. These nodes usually have nonlinear activation functions, e.g. a sigmoidal function. The appropriate weight sets result in a mapping from input signals to desired outputs.

Neural nets are commonly used for pattern classification and functional approximation. Among various neural net models, the single hidden layer feedforward neural net with sufficient hidden nodes can be thought of as a universal function approximator [3, 4]. The neural net can learn a mapping (a functional relationship) between the given inputs and corresponding outputs through training samples.

In this paper, a single hidden layer neural net was trained and tested using visible fringe patterns from a photoelastic plastic shaft coupler as viewed by an optical sensor array (consisting of 32 sensors). The analytic relationship describing the expected fringe pattern resulting from a given torsional strain (shaft torque) is complex and is approximate with regard to boundary conditions and assumptions of planar (2-D) material strain. Since no simple analytic or closed form relationship between inputs (torque) and outputs (observed fringes) exists, this functional mapping problem is ideally suited for neural net signal processing. The average error of this single hidden layer neural net torque sensor is less than 0.4% for stationary shafts and increases with the rotational speed up to 4% at 20 rpm.

2. Description of the Sensor

Rather than directly attaching a photoelastic material to a solid shaft as described in [2], we used a hollow cylinder of photoelastic plastic which is epoxied to aluminum collars which are then attached to the shaft (see Figure 1). We used a commercial polycarbonate plastic with a high strain-optical coefficient. Polarized light from a halogen light source illuminates the plastic cylinder. This polarized light passes through the plastic cylinder, is reflected from a coating of aluminum filled epoxy on the inner surface of the plastic cylinder, and passes through the plastic cylinder a second time. The light incurs an optical phase shift as described by Equation (1) which is dependent upon the strain (caused by the shaft torque) at that point on the sensor plastic cylinder. This optical phase shift is a two-dimensional function of position on the sensor surface. The light reflected from the sensor passes through a polarization filter, which converts the two-dimensional optical phase function to a two-

dimensional intensity function (fringe pattern) such as shown in Figure 2 which can be viewed by an ordinary optical detector.

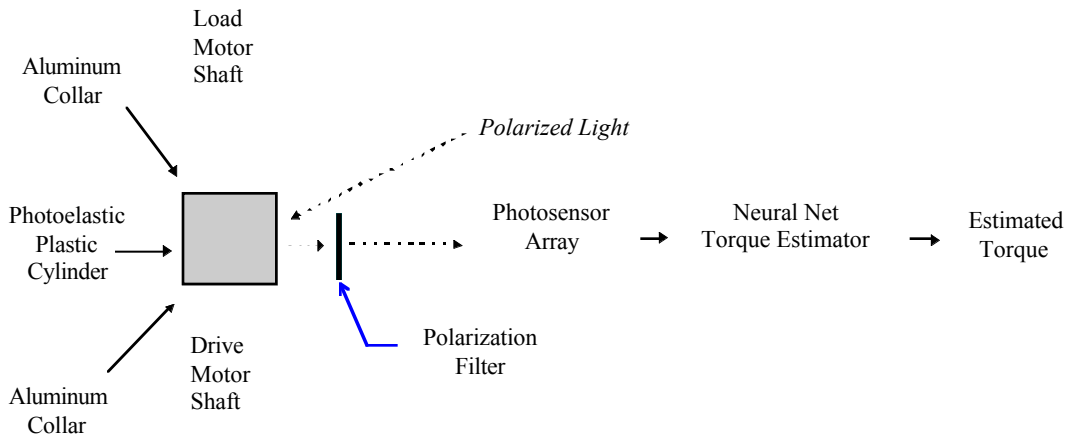


Figure 1. Conceptual Torque Sensor

Figure 3 shows the diagram of an optical torque sensor using the neural net torque estimator. In our experiments, a CCD camera and frame grabber attached to a computer workstation were used to simulate various one- and two-dimensional photo sensor arrays configurations.

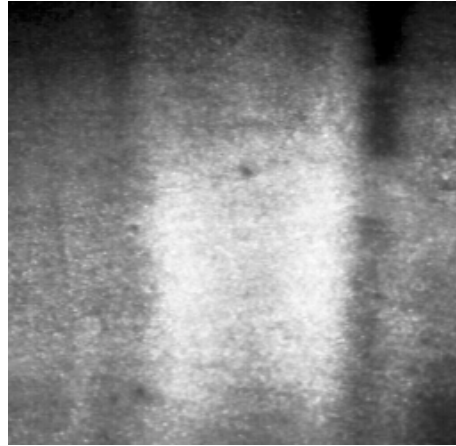


Figure 2. Typical Intensity Pattern of Optical Torque Sensor

3. Experimental Setup

The photoelastic transducer was a hollow cylinder which was mounted to solid motor (drive) and gear train (load) shafts using collets at each end of the cylinder. For static testing of the torque sensor, the load side of the sensor was stationary and torques were applied from the drive side using a computer controlled motor. The shaft torque was measured using a commercial strain gauge torque sensor [S. Himmelstein & Co., MCRT Torquemeter 24-02T (35-1)] with an accuracy of 0.2% which was mounted on the shaft of the motor providing the torque. The load side of the sensor was attached to a Dodge™ right angle gear box which was connected to a computer controlled load motor. Under computer control this apparatus provides accurate computer controlled torques both for stationary (static) and rotating (dynamic) shaft operation [5].

Figure 3 shows the experimental setup used for data acquisition. The CCD camera was perpendicular to the shaft axis. A commercial 120-volt halogen lamp was used to

illuminate the sensor from an angle of about 10° - 20° from the normal. A sheet of commercial polarizing plastic was used as the filter. Both linear and circular polarizing filters were used with little, if any, measurable difference in torque sensor performance between the two.

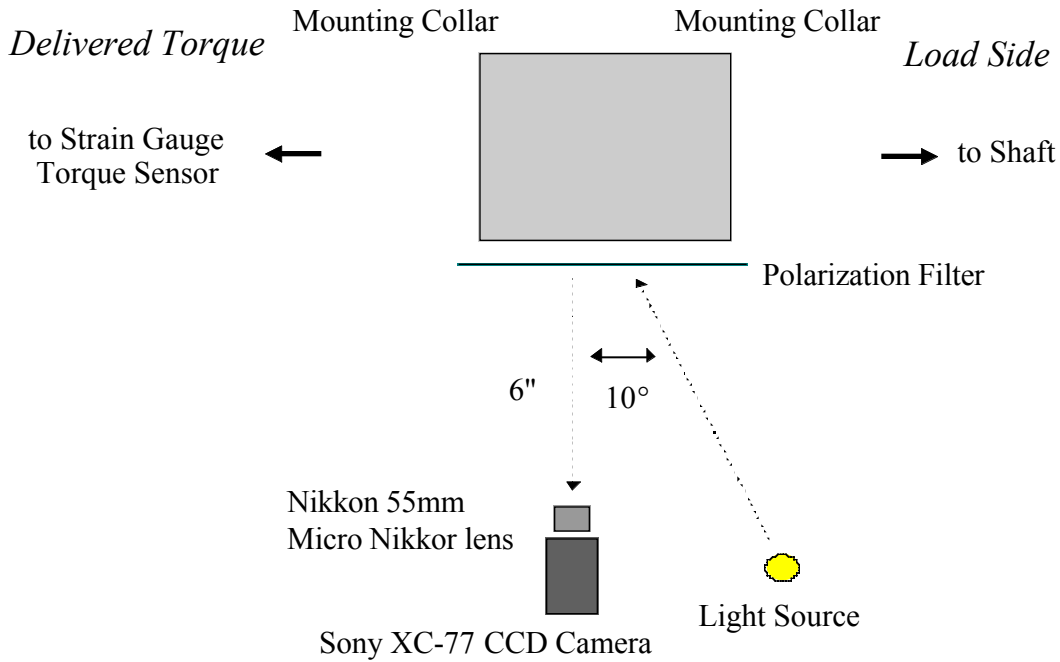


Figure 3. Schematic of Experimental Setup

4. Image Processing

All images were recorded using a Sony XC-77 512x480 pixel CCD camera interfaced to a Matrox MVP frame grabber. A Nikon 55mm Micro-Nikkor lens was used to image the fringe patterns on the photoelastic cylinder.

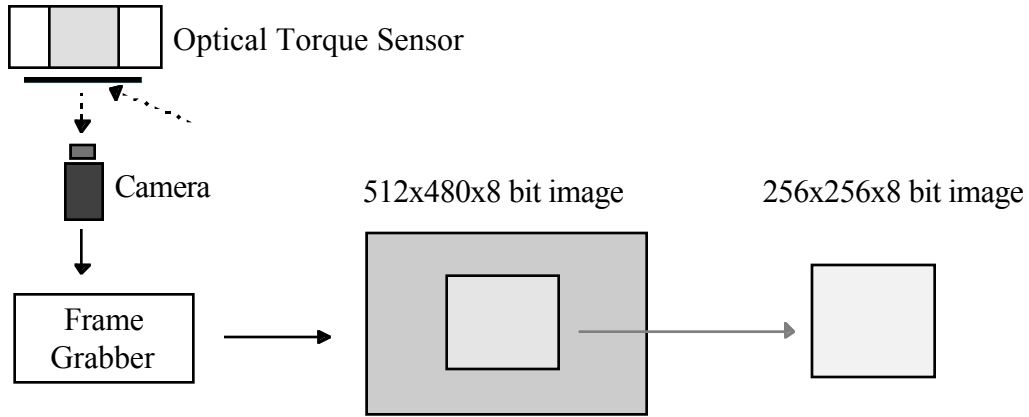


Figure 4. Image Acquisition

Because only the surface of the photoelastic plastic cylinder (and not the collar) was of interest, the image was cropped to 256x256 pixels.

5. Neural Net Processing

A standard feedforward, backpropagation neural net was the basis for all torque estimation. Neural nets can compute any computable function [3, 4]. Anything that can be represented as a mapping between vector spaces can be approximated to arbitrary precision. In practice, neural nets are useful for mapping problems which are tolerant of errors, have example data available, but to which hard and fast rules can not easily be applied. They are particularly useful for non-linear mappings such as that between the measured shaft torque and the intensity patterns observed on the photoelastic shaft coupler.

In these experiments, the neural net is used to learn the mapping between the optical fringe pattern seen by the camera and the shaft torque, as measured by the strain gauge torque sensor. There was no known analytical relationship between a given input and an estimated output.

The connection strengths (weights) between nodes are initially assigned to small random numbers before training. Training using backpropagation [6] then proceeds by repeating the training pairs (values from the image arrays as inputs, corresponding shaft torques as outputs) until a satisfactory level of performance (typically 10^{-6} mean squared error) is reached.

Backpropagation computes the partial derivatives of error with respect to the neural weights. With these partial derivatives, it is possible to perform gradient descent search in weight space. If small steps are taken in the direction of the gradient, the error is guaranteed to reach a local minimum. This local minimum has been empirically accepted as a good enough solution for most purposes, although it is a very slow, time consuming process.

For a practical sensor it is desirable to train the neural net in the shortest possible time. This requires taking the largest possible steps in the direction of the gradient without overshooting the minimum error solution. A set of partial derivatives collected at a single point does not have enough information for deciding step size. If the higher-order derivatives (the curvature of the error function) are available, it is possible to choose better, or larger step size more safely.

A variation of backpropagation, called the quickpropagation training algorithm assumes each weight in the neural net has a quadratic error curve [7]. Each weight in the net is assumed to affect the error independently of the others. The quadratic calculation is then approximated using a difference of gradients between the current and the previous epoch.

Special provisions must be made for starting the algorithm, what to do when the last weight changes are zero, and what to do when the current derivative is greater than the

previous derivative. The quickpropagation technique works well in practice, and considerably shortens the training time than the traditional backpropagation algorithm.

The optical intensity image from the camera was input to a neural net to estimate the shaft torque. The motivation for using a neural net to process the image is that neural nets are excellent functional estimators and should be able to learn the functional mapping from intensity patterns to shaft torque. However, a 256x256 pixel image represents more than a fifty-thousand sensor elements – far too many to directly input to a neural net. In an effort to reduce the number of inputs to the neural net and to more accurately represent realizable sensor arrays, various strips of pixels were used as inputs to the neural net, as shown in Figure 5. Each strip contained 32 sensor cells where each cell consisted of a square array of 32x32 image pixels as shown in Figure 6. All the pixels in each cell are averaged to produce a single input to the neural net corresponding to each cell. All pixels outside the cell boundaries were ignored. Several other methods of image pre-processing were also tested. In one method, the central 48 bins of a 64 bin histogram of the entire 256x256 pixel image were used as inputs to the neural net. In yet another scheme, red, green and blue filters were used to simulate a color sensor. This was motivated by the colored fringes produced by the white light source.

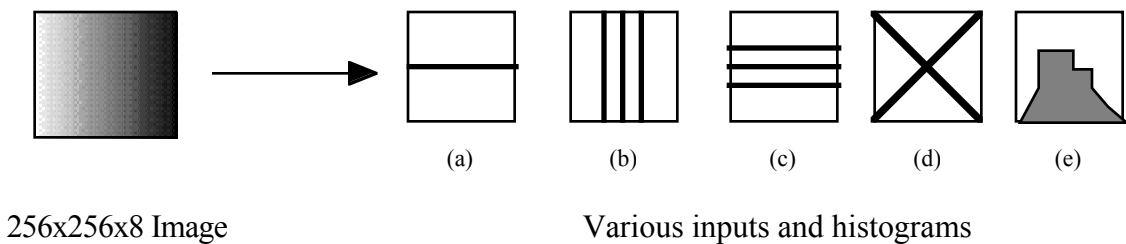


Figure 5. Various Pre-processing Schemes of 256x256x8 image

For this optical torque sensor, the neural net was a standard backpropagation net with 32 to 96 input nodes (corresponding to the outputs from the optical sensor), 12 nodes in a single hidden layer and a single output node for the estimated torque. The quickpropagation algorithm was used for faster learning [7]. The neural net was then trained to estimate the applied torque from the supplied fringe pattern. The training pairs consisted of 32 to 96 element sensor array intensity vectors corresponding to an experimentally obtained fringe pattern from the birefringent sensor, and a corresponding torque value as measured by the strain gauge shaft torque sensor.

The performances of the pre-processing schemes of Figure 5 using a single hidden layer neural net are summarized in Table 1. For these static experiments the torque was varied over the range 70 - 150 lb-in torque. All strips contained 32 or 48 sensors, depending on configurations. The testing and training errors in Table 1 were averaged over the 70 - 150 lb-in range. Among these pre-processing schemes, the single horizontal strip with 32 cells of 32x32 pixels gave the best results and was consequently used for all the experiments conducted in Section 6. It is interesting to note that the simulated color camera (Table 1(f)) provided no substantial improvement over the gray scale image (Table 1(a)).

Configuration (neural net architecture)	Typical NN Training Error	Typical NN Testing Error
(a) 1 Horizontal Strip (32 input nodes; 15 hidden nodes)	0.16%	0.38%
(b) 3 Vertical Strips (48 input nodes; 15 hidden nodes)	0.22%	0.58%
(c) 3 Horizontal Strips (48 input nodes; 15 hidden nodes)	0.18%	0.40%
(d) 2 Diagonal Strips (32 input nodes; 15 hidden nodes)	0.26%	0.72%
(e) Histogram Inputs (48 input nodes; 15 hidden nodes)	0.65%	1.50%
(f) 1 Horizontal strip using RGB filters (48 input nodes; 15 hidden nodes)	0.20%	1.20%

Table 1. Neural Net Training/Testing Results for the Preprocessing Schemes of Figure 5.

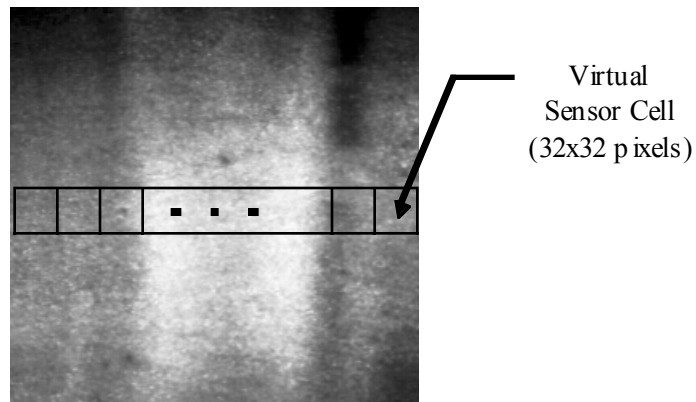


Figure 6. Pre-processing of 256x256x8 image

6. Experimental Results

The procedure of evaluating a sensor involved two steps: training the neural net for a specified image pre-processing scheme, and then testing the neural net using the same pre-processing scheme. In the training phase, a series of sensor images corresponding to a sequence of commanded torques is acquired by the camera/frame grabber, preprocessed, and input to the neural net. The typical training time for the neural net to achieve a mean squared error of 10^{-6} using the quickpropagation algorithm was under 2 minutes using a HP 9000/712 workstation. The testing of the sensor involves applying a known torque to the sensor and comparing the torque estimated by the neural net output to the actual torque.

Figure 7 and 8 show the training and testing results when 41 torque values representing 0 to 200 lb-in in 5 lb-in increments were used to train and test the neural net. The neural net output (represented by x's) is superimposed on the known torque value (represented by rectangles) and the difference (error) is shown by the circles as a percentage of the actual torque. The average training error of 8% and average test error of 13.8% are not good results compared to later experiments. These large errors were due to attempting to train the neural net over a torque range of 0 - 200 lb-in. At low torque values, there was not enough change in the fringe patterns to be recognized by the neural net torque estimator. Restricting the torque values to those between 70 and 150 lb-in greatly improved the neural net accuracy.

Neural Net Torque Estimator (Training)

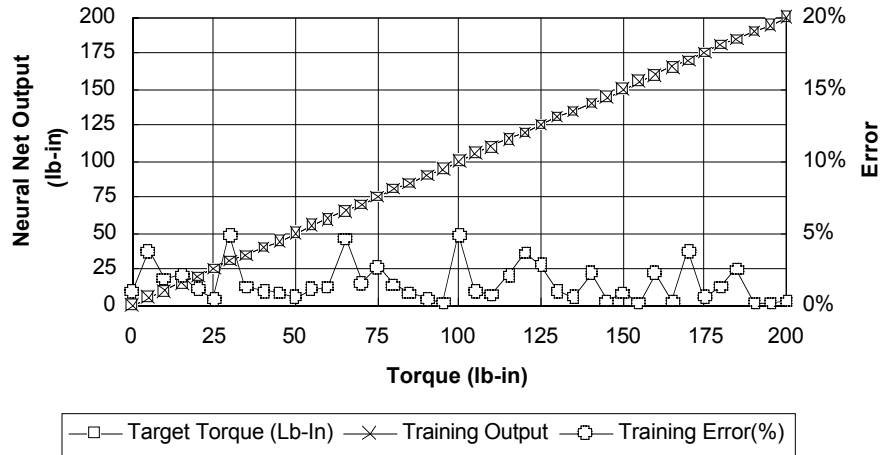


Figure 7. Torque Sensor Training Results over 0 to 200 lb-in

Neural Net Torque Estimator (Test)

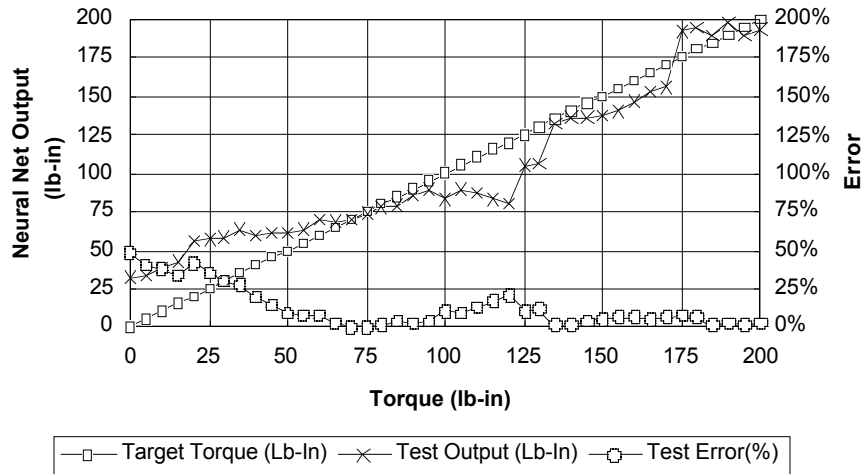


Figure 8. Torque Sensor Testing Results over 0 to 200 lb-in

Figures 9 and 10 show the training and testing results for this restricted torque range. In Figure 9 the neural net output (represented by x's) is superimposed on the known torque value (represented by rectangles) and the difference (error) is shown by the circles as a

percentage of the actual torque. Forty-one torque values representing 70 to 150 lb-in in 2 lb-in increments were used to test the sensor.

In Figure 10 the neural net output (represented by x's) is superimposed on the known torque values (represented by rectangles) and the difference (error) is shown by the circles as a percentage of the actual torque. Forty-one torque values representing 70 to 150 lb-in in 2 lb-in increments were used to train the net. The average testing error (0.38%) were larger than the average training errors (0.16%). These numbers were typical of all polycarbonate sensors we tested.

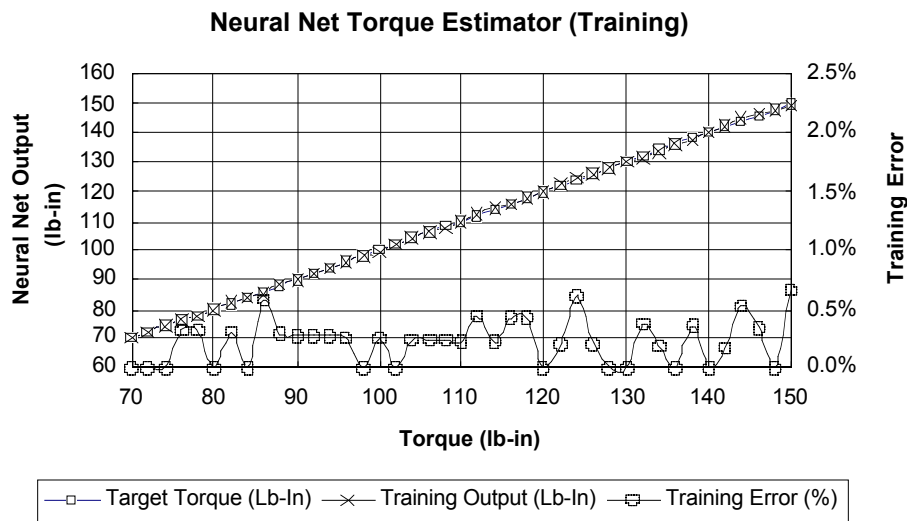


Figure 9. Performance of Neural Net Torque Estimator (Training)

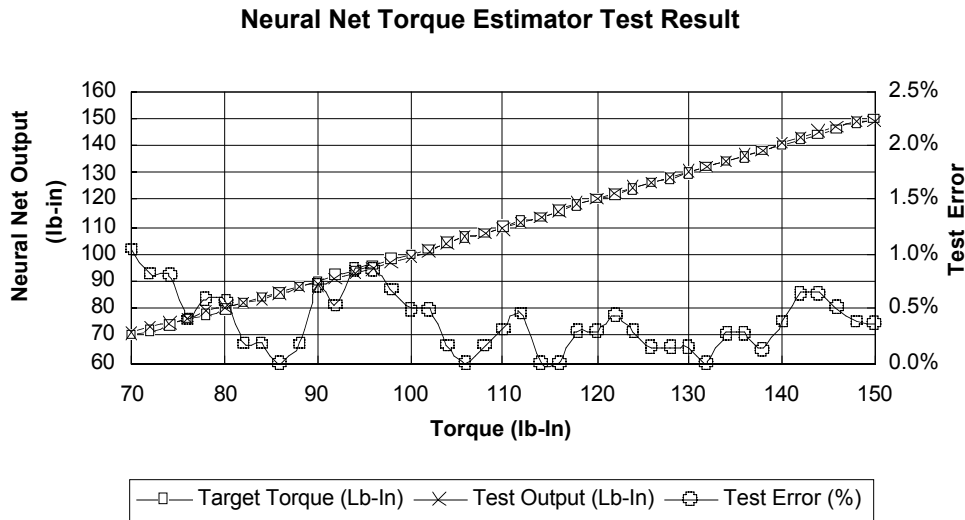


Figure 10. Performance of Neural Net Torque Estimator (Test)

The same type of experiment was repeated for slowly rotating shafts, i.e., 1 radian/second and 4 radians/second. These experiments were characterized by random vertical displacements of the fringe patterns in the acquired images (*vertical jitter*) and a decreasing contrast of the fringe patterns as the rotational speed increased (*smearing effect*). Vertical jitter was due to a lack of synchronization between the CCD camera and the rotating shaft. This jitter was removed by using a reference mark on the sensor mount and appropriate image processing (registration) to insure that the sensor inputs always came from the same physical locations on the sensor surface. The image smearing was determined to be due to image interleaving in the frame grabber and was removed by restricting the data to a single image field. The sensor data was then processed in the same manner as for a static experiment. Typical processed images with jitter and smearing removed are shown in Figure 11. The circular objects in Figure 11 are registration marks.



(a) 80 LB-In

(b) 110 LB-In

(c) 140 LB-In

Figure 11. Typical Processed Images at 2 radians/second

Figure 12 shows the sensor test results at 1 radian/second shaft speed. The neural net outputs (represented by \diamond 's and \times 's, receptively) are superimposed on the known torque value (represented by rectangles) and the differences (error) shown by the circles and triangles as percentages of the actual torques. The average training error was 0.6% and the average testing error was 0.4% at this shaft speed. At these low rotational speeds, there was no significant difference between dynamic and static testing of the sensor.

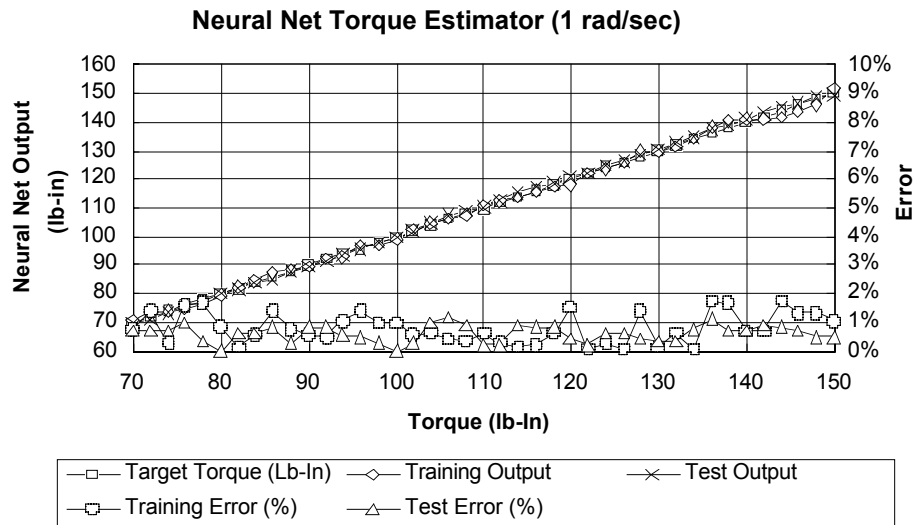


Figure 12. Training/Testing Result at 1 rad/sec

Figure 13 shows the sensor test results at 4 radian/second shaft speed. The neural net outputs (represented by \diamond 's and \times 's, receptively) are superimposed on the known torque value (represented by rectangles) and the differences (error) are shown by the circles and triangles as percentages of the actual torques. The average training error was 0.2% and the average testing error was 3.5% at this speed. In general, as the sensor rotational speed increased, the testing error also increased.

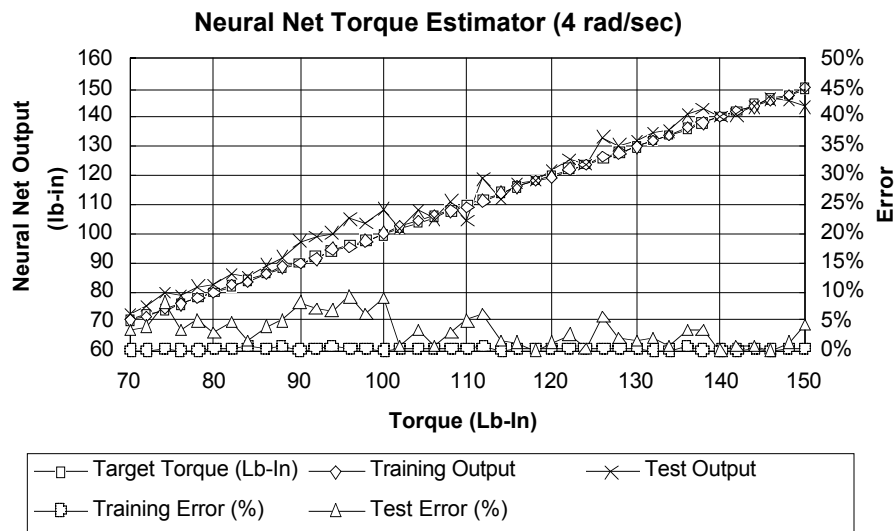


Figure 13. Training/Testing Result at 4 rad/sec

7. Discussion and Conclusion

The neural net based birefringent torque sensor has shown its ability to accurately measure shaft torque values over limited torque ranges. The neural net torque estimator described has demonstrated less than 0.4% average estimation error over a 70 - 150 lb-in static torque range. This excellent torque measurement accuracy shows the potential for accurately measuring torques by means of non-contacting optical sensor arrays. The images used in these

experiments are equivalent to those obtainable using a simple linear array of photodetectors with a considerable reduction in system complexity.

References

1. Kobayashi, A. S., *Handbook on Experimental Mechanics*, 2nd rev. Ed., VCH Publishers Inc., 1993.
2. "Introduction to Stress Analysis by the Photo Stress Method," Tech Note TN-702-1, Measurements Group, Inc., 1989.
3. Hornik, K., M. Stinchcombe, and H. White, "Multilayer Feedforward Networks are Universal Approximators," in *Neural Networks*, vol. 2, pp. 359-369, 1989.
4. Funahashi, K., "On the Approximation Realization of Continuous Mappings by Neural Networks," in *Neural Networks*, vol. 2, pp. 183-192, 1989.
5. Newman, W. S., "Comparative Evaluation of Three Transmission Types: Worm Gear, Cone Drive and Traction Drive," in *CAISR Technical Report 93-109*, Center for Automation and Intelligent Systems Research, Case Western Reserve University, 1993.
6. Rumelhart, D. E., Hinton, G. E., and Williams, R. J., "Learning Internal Representations by Error Propagation," in Rumelhart, D. E. and McClelland, J. L. (editor), *Parallel Distributed Processing: Explorations in the Microstructure of Cognition*, chapter 8. MIT Press, 1986.
7. Fahlman, S. E., "Faster Learning Variations on Back Propagation: An Empirical Study," in *Proceedings of the 1988 Connectionist Models Summer School*, San Mateo, CA, Morgan Kaufmann Publishers, 1988.